Macromolecules
ARTICLE

Macromolecules **2009**, *42*, 6193–6201 **6193**
DOI: 10.1021/ma9009406

Tailoring Core−Shell Polymer-Coated Nanoparticles as Block Copolymer Surfactants

Bumjoon J. Kim,[†] Glenn H. Fredrickson,[‡,∥,§] Joona Bang,[⊥] Craig J. Hawker,[∥,§] and Edward J. Kramer*[,‡,∥,§]

[†]*Department of Chemical and Biomolecular Engineering, Korea Advanced Institute of Science and Technology, Daejeon, 305-701, Korea,* [‡]*Department of Chemical Engineering* [§]*Materials Research Laboratory* [∥]*Department of Materials, University of California, Santa Barbara, California 93106, and* [⊥]*Department of Chemical and Biological Engineering, Korea University, Seoul 136-701, Korea*

Received April 30, 2009; Revised Manuscript Received June 20, 2009

ABSTRACT: The effect of core−shell polymer-coated nanoparticles on block copolymer morphology is investigated systematically by controlling particle positioning within a block copolymer template. Our approach of varying the areal chain density (Σ) of short thiol terminated polystyrene (PS-SH) brushes on the particles where the molecular weight (M_n) of the PS ligands (2.5 kg/mol) is used to control the fraction of the particles adsorbed to the interface of PS-*b*-P2VP diblock copolymer domains (M_n = 196 kg/mol). The change in Σ from 2.38 to 0.49 chains/nm^2 brings systematic control over the fraction of Au particles bound to the PS/P2VP interface (f_i), this fraction ranging from 0 to 95%. Particles with Σ of 2.38 chains/nm^2 ($f_i \sim 0$) were observed to localize within the PS domains and further produce a macroscopic particle aggregated phase separate from the PS-*b*-P2VP mesophase. In contrast, decreasing the Σ of PS chains provides for strong binding of Au nanoparticles to the PS/P2VP interfaces as a consequence of preferential wetting of one block of the copolymer (P2VP) to the Au substrate. Interestingly, the addition of low volume fractions (ϕ_P) of such nanoparticle surfactants (Σ < 1.1 chains/nm^2) to lamellar diblock copolymers initially leads to a decrease in lamellar thickness, a consequence of decreasing interfacial tension, up to a critical value of ϕ_P beyond which the block copolymer adopts a bicontinuous morphology. The relationship between domain spacing and morphology of block copolymer with the level of nanoparticle surfactants will be discussed based on a strong-segregation model. In addition, the rational design of nanoparticle surfactants based on the nature and density of the grafted chains will be described.

Introduction

Bicontinuous (or, more generally, cocontinuous) polymer morphologies have a wide range of current and potential applications. Cross-linked interpenetrating networks, for example, are well-known to have unique combinations of mechanical properties, such as simultaneously high modulus and toughness.[1,2] As another example, when one phase of a bicontinuous composition is removed to create a porous structure, the remaining continuous phase provides a rigid self-supporting scaffold that can be used in separations, in catalysis, and as absorbent or thermal management materials.[3−5]

Surveying the field of phase-separated copolymers, one of the most rapidly growing areas for bicontinuous polymer structures, involves thin films rather than bulk materials. An example is bulk heterojunction organic photovoltaic films where interpenetrating electron transporting and hole transporting conjugated polymer phases can bring a significant increase in the interfacial area which allows for efficient exciton dissociation and leads to improved solar cell efficiencies.[6−8] Bicontinuous alloys with one of the polymer components a π-conjugated polymer can also be useful as conductive coatings for EM shielding or for corrosion resistance. In the context of thicker films, bicontinuous ion transporting membranes are of interest in fuel cells and battery applications.

While bicontinuous polymer structures are highly desirable, robust strategies for creating thermally stable bicontinuous morphologies are rather limited.[9−13] Upon melt mixing or casting from a common solvent, most binary polymer blends are thermodynamically immiscible and undergo macrophase separation. The morphology that is obtained is usually monocontinuous (e.g., drops of phase A in a matrix of B) and depends very much on the thermal or solvent processing conditions to which the blend is subjected. Furthermore, unfortunately such a procedure does not lend itself to subsequent polymer melt processing, since the bicontinuous morphology will be lost upon remelting and melt processing, e.g., by injection molding to achieve a prescribed shape.

Nanoparticles as well as colloidal particles can act like surfactant molecules, particularly if adsorbed to an immiscible fluid−fluid interface.[14] Such "particle surfactants" can be active or passive in conferring special properties to the composition and have been demonstrated to help create emulsions by decreasing the interfacial tension and stabilizing the liquid film between droplets, thus preventing coalescence.[14−16] Simulations[17,18] and experiments[19−22] have shown that nanoparticle surfactants can stabilize bicontinuous emulsions of small molecule liquids as well as bicontinuous morphologies in blends of A and B homopolymers. These studies assume such emulsions to be metastable, with an initial bicontinuous microstructure resulting from spinodal decomposition of the liquid or polymer mixture being arrested by the "jamming" of nanoparticles strongly adsorbed to the liquid/liquid or polymer/polymer interfaces.

Precise positioning of particles at the interface between two different polymers is required to achieve surfactant-like

*To whom correspondence should be addressed. E-mail: edkramer@mrl.ucsb.edu.

Published on Web 07/24/2009

properties, and a recent strategy for controlling the location of nanoparticles in a block copolymer or polymer blend involves tuning the surface properties of nanoparticles by end-attaching ligands such as organic small molecules,[23−28] homopolymers,[19,29−34] a mixture of homopolymers,[35] random copolymers,[36] and diblock copolymers[37] to the nanoparticle surface. Once particles are "neutral" and the interfacial tension between two different domains of diblock copolymers or the separate phases of homopolymer blends is sufficiently large, particles will segregate to the interface between two phases.[38−41] In our recent experiments we observed that the formation of a diblock copolymer bicontinuous morphology can be induced using a two-component system consisting of a symmetric poly(styrene-*b*-2-vinylpyridine) diblock copolymer (PS-*b*-P2VP) and nanoparticle surfactants.[42] The bicontinuous morphology can be produced over a wide range of particle volume fractions. Furthermore, the uniform bicontinuous structure with characteristic dimensions well below 100 nm is ideal for many thin film applications.

In the initial experiments, Au nanoparticles covered with a single low areal chain density Σ of low molecular weight polystyrene thiol (PS-SH) ligands were used as the nanoparticle surfactant. In this paper, the effect of changing the areal chain density Σ of the PS-SH ligands on the morphology of symmetric PS-*b*-P2VP block copolymers is investigated systematically. Since P2VP segments are preferentially attracted to the bare gold nanoparticle surface over PS segments, changing Σ of the PS-SH ligands on the Au nanoparticles can produce various fractions (f_i) of particles segregated to the PS/P2VP interface (i.e., $f_i \sim 0$ for the case where all particles are dispersed near the center of the PS domains and $f_i \sim 1$ for the case where all particles are localized at the interfaces). By varying Σ, a range of intermediate f_i values can be accessed such that some of the particles are dispersed near the center of the PS domains while others are located at the interface. As will be described below, we believe that this dispersion in particle location is a consequence of a Poisson distribution of the number of brush chains among particles.[43] A phase diagram representing the morphology of PS-*b*-P2VP block copolymers ($M_n \sim 196$ kg/mol) containing PS-coated Au nanoparticles as a function of the particle volume fraction (ϕ_P) and Σ has been established. In addition, the segregation of nanoparticle surfactants to the block copolymer interface leads to a decrease in interfacial tension between the two blocks of block copolymer and thus causes a decrease in the domain spacing. We show that the measured domain spacing is a unique function of the volume fraction of particles segregated to the interface. The domain spacing and the threshold for the transition of morphology from lamellar to bicontinuous morphology are further compared to the predictions of a strong-segregation theory.

Experimental Section

Synthesis of Thiol-Terminated PS (PS-SH) and Random Copolymers of Styrene and 2-Vinylpyridine (PS-*r*-P2VP-SH). A symmetric poly(styrene-*b*-2-vinylpyridine) (PS-*b*-P2VP) diblock copolymer with total molecular weight $M_n \sim 196$ kg/mol and a polydispersity (PDI) of 1.11 (Polymer Source, Inc.) was used as the block copolymer template in which to investigate systematically the position of gold nanoparticles. To incorporate gold nanoparticles into PS-*b*-P2VP block copolymer template, the particles were stabilized by thiol-terminated PS (PS-SH). PS-SH was synthesized by living anionic polymerization as described elsewhere.[29,36] The molecular masses M_n of the thiol terminated PS polymers (PS-SH) were determined to be 2.5 kg/mol with PDI of 1.1, measured by size exclusion chromatography (SEC) calibrated by PS standards. Thiol-terminated random copolymers of styrene and 2-vinylpyridine (PS-*r*-P2VP-SH) were synthesized by reversible addition−fragmentation transfer (RAFT) procedures using a dithioester RAFT agent and AIBN at 70 °C.[36,44] The polymer end group was converted to a thiol group by reaction with hexylamine. The conversion during the RAFT polymerization was kept to 12% in order to prevent composition drift caused by the difference in the reactivity ratio of the styrene and 2-VP monomers. The M_n and PDI of PS-*r*-P2VP were 3.5 kg/mol and 1.1, respectively, with a mole fraction of styrene in the PS-*r*-P2VP measured to be 0.5 by ^{1}H NMR.

Table 1. Characterization of Gold Nanoparticle Coated by PS Chains (M_n = 2.5 kg/mol) Synthesized with Various Initial Mole Ratio of PS Chains to (PS Chains + Gold Atoms) (f_{PS})

list	particle core diameter (nm)[a]	particle diameter (core + shell) (nm)	areal chain density Σ (chains/nm^2)
Au-PS 2.38	2.5 ± 0.8	7.3	2.38
Au-PS 1.46	2.4 ± 0.7	6.2	1.46
Au-PS 1.06	2.2 ± 0.7	5.3	1.06
Au-PS 0.97	2.6 ± 0.6	5.7	0.97
Au-PS 0.92	2.8 ± 0.8	6.0	0.92
Au-PS 0.73	3.0 ± 0.7	5.8	0.73
Au-PS 0.49	3.0 ± 0.7	5.2	0.49
Au-PS-*r*-P2VP[b]	3.0 ± 0.7	8.1	1.61

[a] Obtained from image analysis based on TEM images for at least 300 particles. [b] PS-*r*-P2VP-SH (M_n = 3.5 kg/mol).

Synthesis of PS-Coated Au Nanoparticles (Au-PS). The synthesis of PS-coated Au nanoparticles was accomplished using a two-phase method[45] consisting of toluene and water by varying the initial mole feed ratio of PS ligands to (Au atoms + PS ligands) (f_{PS}) from 1/3 (= 0.33) to 1/33 (= 0.03). The polymer-coated gold particles were separated from unattached PS-thiol by precipitation using a mixture of ethanol and toluene, concentrating the particles by centrifugation followed by membrane filtration (MWCO 30 000 Da, Millipore, Inc.) using dimethylformamide, dioxane, and methanol to remove ungrafted ligands as well as any residual reducing agent. The characteristics of these polymer-coated gold nanoparticles are summarized in Table 1. The gold core diameter distribution obtained as a histogram from TEM image analysis was used to calculate the average surface area per gold nanoparticle. Weight fractions of gold and polymer ligands were measured by thermal gravimetric analysis (TGA). These numbers were confirmed by elemental analysis. The weight fractions of the polymer chains were converted into volume fractions using the density of the polymer (∼1.05 g/cm^3) and the density of gold (∼19.3 g/cm^3). The number of polymer ligands per gold particle for various core−shell type particles, divided by the average surface area of the gold particle, gives the mean areal chain density (Σ) of polymer ligands on the particle surface. For convenience the following labeling is used: PS-Au 2.38, PS-Au 1.46, PS-Au 1.06, PS-Au 0.97, PS-Au 0.92, PS-Au 0.73, and PS-Au 0.49 denote PS-coated Au nanoparticles with Σ = 2.38, 1.46, 1.06, 0.97, 0.92, 0.73, and 0.49 chains/nm^2, respectively. The synthesis of PS-*r*-P2VP-SH-coated Au nanoparticles was performed using a one-phase method in THF as described elsewhere.[46]

Preparation of PS-*b*-P2VP/Polymer-Coated Au Nanoparticle Composites. To prepare the nanocomposite films, a 1−2 wt % block copolymer solution in dichloromethane, which is a neutral solvent for the PS and P2VP blocks,[30] was mixed with PS-coated gold nanoparticles to produce various particle volume fractions ranging from 0.01 to 0.53 in the final block copolymer/nanoparticle film. A particle/block copolymer composite was prepared by solvent-casting a mixture of PS-Au nanoparticles and PS-*b*-P2VP block copolymer in dichloromethane onto an epoxy substrate and then annealing under a saturated solvent atmosphere at 25 °C for at least a day. All solvent in the sample was allowed to evaporate very slowly during over an additional day. Samples were subsequently dried in the air overnight and further under vacuum for 4 h to make sure that no solvent was left in the

sample. As a result, a 10−20 μm thick film of nanoparticle/block copolymer composite was produced.

Characterization. The diameter and the location of the PS-coated gold particles (PS-Au) in the PS-*b*-P2VP matrix were determined by transmission electron microscopy (TEM) using a FEI Tecnai G2 microscope operated at 200 kV. PS-Au nanoparticles were dissolved at a very low concentration in dichloromethane or THF. A 20−30 nm thick carbon film-coated TEM grid was dipped into the solution for a second, dried in the air, and then examined by TEM. Samples of gold nanoparticle−block copolymer composites were prepared for cross-sectional TEM by microtoming epoxy-supported films into 25−40 nm thick slices that were then stained by exposing them to iodine vapor for a short time to visualize the particles at the PS/P2VP interface clearly while maintaining contrast between PS and P2VP domains. While the TEM micrographs provide direct evidence of particle location as a function of the areal chain density, errors in the particle distribution within a polymer block domain may be caused by tilt of the lamellar interfaces relative to the TEM beam direction, so that the interfaces appear broader and the domains narrow in the projected image. Care was taken to reduce such errors, both by carefully tilting the sample so as to minimize the interface width and by analyzing a large number of particles (at least 500 particles) collected from different samples at each given areal chain density.

Results

Polystyrene-coated gold nanoparticles of approximately the same core diameter were synthesized with the areal chain density Σ of PS-SH ligands on the nanoparticles ranging from 2.38 to 0.49 chains/nm^2 (Table 1). The decrease in Σ has the effect of increasing the attractive interaction between the bare Au surface not shielded by the PS-SH ligands and the P2VP block of the diblock copolymer. The nanoparticle Au core diameter as well as an estimate of the overall diameter of the PS-coated nanoparticles including the shell thickness of PS is shown as a function of Σ in Figure 1. The average particle core (Au) diameter for each synthesis was determined from TEM images by analyzing at least 300 particles using standard image analysis software (Image Pro). As Σ decreases from 1.46 to 0.49 chains/nm^2, the particle core diameter increases slightly from 2.4 to 3.0 nm. However, the overall particle (core + shell) diameter remains constant at about 5.7 nm due to the smaller number of PS chains on the nanoparticles with smaller Σs and larger core diameters. Theory[32] and simulation[40,41,47] as well as experiments[23,32] suggest that particle diameter is one of most important factors influencing particle positioning in a block copolymer matrix since the adsorption energy of particles to the interface between block copolymer domains is proportional to the square of the block copolymer interfacial area occupied by the cross section of nanoparticle.[39] In addition, the diameter should also influence particle positioning by imposing an entropic penalty on the copolymer chains that cannot penetrate far into the particle. Therefore, keeping the mean diameter of the particles roughly constant is a prerequisite to allow one to investigate systematically the effect of polymer ligand areal density, its effect on the segregation of the particles to the interface, and the effect of this segregation on the block copolymer morphology.

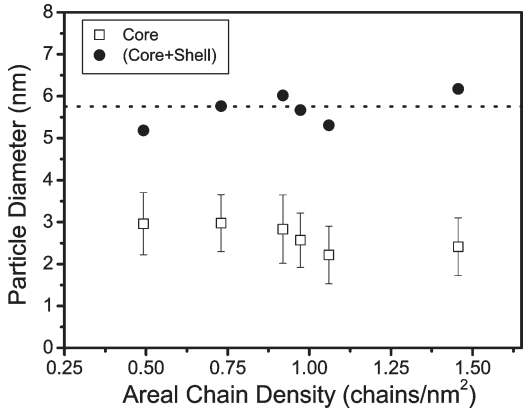

Figure 1. Diameter of Au particle core as well as that of the (core + shell). These particles were coated with various areal chain densities (Σ) ranging from 0.49 to 1.46 chains/nm^2 of PS-SH chains (M_n = 2.5 kg/mol). As Σ is decreased, the particle core diameter is increased slightly due to the lower density of PS chains on the nanoparticle. However, the overall particle (core + shell) diameter is nearly constant at 5.7 ± 0.5 nm.

Figure 2 reveals the Σ effect of PS-SH chains on the surface of various PS-Au particles on the morphology of symmetric PS-*b*-P2VP block copolymers. Figures 2a,b show the cross-sectional morphology of PS-*b*-P2VP block copolymers mixed with gold particles having Σ of 2.38 chains/nm^2 (PS-Au 2.38). At a relative low particle volume fraction (ϕ_P = 0.09), the gold particles are dispersed in the PS domain (lighter phase) of a

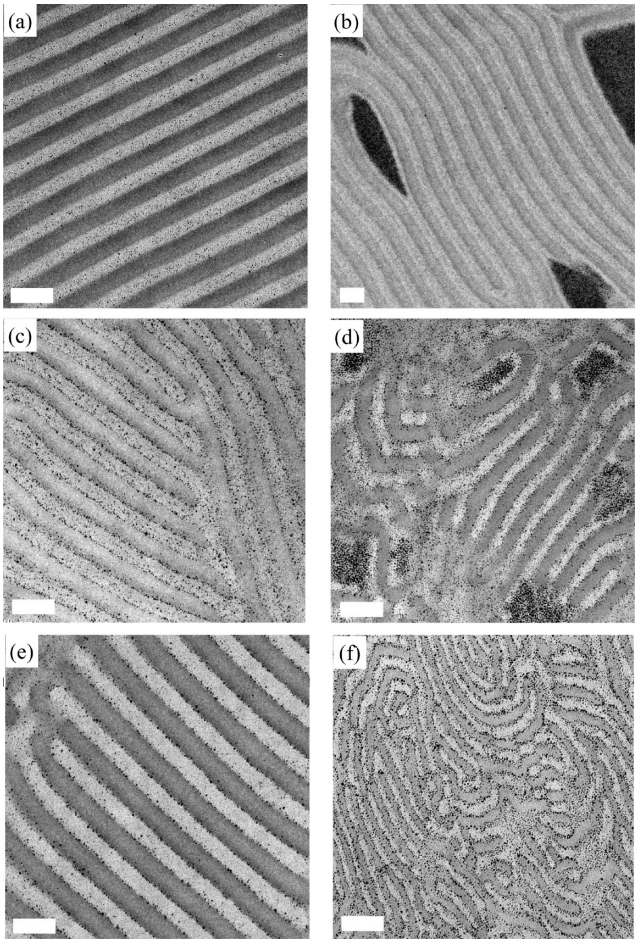

Figure 2. Cross-sectional TEM images showing the effect of PS-SH areal chain density that controls the nanoparticle location on the morphology of a symmetric PS-*b*-P2VP block copolymers (M_n = 196 kg/mol). PS-*b*-P2VP morphology mixed with PS-Au 2.38 nanoparticles (Σ = 2.38 chains/nm^2) having a volume fraction (ϕ_P) of (a) 0.09 and (b) 0.25. PS-*b*-P2VP mixed with PS-Au 1.46 gold nanoparticles (Σ = 1.46 chains/nm^2) having ϕ_P of (c) 0.07 and (d) 0.23. PS-*b*-P2VP mixed with PS-Au 1.06 gold nanoparticles (Σ = 1.06 chains/nm^2) having (e) ϕ_P = 0.03 and (f) ϕ_P = 0.20. In (b), at ϕ_P = 0.25, lamellar domains with a low volume fraction of gold nanoparticles are seen together with macrophase-separated gold nanoparticle rich regions (very dark). In contrast, at a similar ϕ_P = 0.20, (f) shows the disrupted block copolymer domains with the reduced domain size without any macrophase-separated gold nanoparticle-rich regions. Scale bar in each micrograph is 100 nm.

well-aligned lamellar morphology as shown in Figure 2a. As the ϕ_P is increased to 0.25, the TEM image shows that large regions of aggregated nanoparticles are present at this nanoparticle loading, indicating coexistence between a macrophase that is highly enriched in nanoparticles and a lamellar mesophase with a much lower nanoparticle concentration. In contrast, the TEM image of the block copolymer morphology containing PS-Au 1.06 particles at a low nanoparticle loading ($\phi_P \sim 0.03$) (Figure 2e) shows that most nanoparticles are segregated to the PS/P2VP interfaces in the well-ordered lamellar morphology. Of particular interest is that Figure 2f shows that the interfacially active nanoparticles PS-Au 1.06 cause a dramatic change in the morphology of the composite at a nanoparticle loading of $\phi_P \sim 0.20$. There is no sign of macrophase separation, and moreover, the nanoparticles have caused a uniform disruption of the block copolymer lamellar phase and have decreased its domain spacing h.

The morphology of the PS-*b*-P2VP block copolymer containing PS-Au 1.46 particles, thus an intermediate Σ value between those of the two particles discussed above, seems to experience both transitions caused by PS-Au 2.38 and PS-Au 1.06 nanoparticles. A lamellar mesophase of PS-*b*-P2VP containing gold particles located at both PS/P2VP interfaces and in the PS domain is observed at relative low $\phi_P \sim 0.07$ as shown in Figure 2c. At a larger ϕ_P of 0.23, the aggregation of gold particles between lamellar sheets is observed in Figure 2d. At the same time, however, the lamellar order of the PS-*b*-P2VP phase is disturbed due to the particles localized at the PS/P2VP interface, and therefore, the morphology shown in Figure 2d includes some of the characteristics of both Figures 2b,f. However the regions of macrophase-separated particle-rich phase in the PS-*b*-P2VP lamellar phase shown in Figure 2d are much smaller than those in Figure 2b at the comparable ϕ_P, suggesting the driving force for macrophase separation or its kinetics are much less in this case. The small regions of macrophase-separated particle aggregation seem to stabilize and/or create defects and grain boundaries in the block copolymer domains, which is consistent with the experimental results of Listak and Bockstaller.[31]

To understand the effect of the PS-SH ligand Σ of the PS-Au particles on the block copolymer morphology, we first investigate systematically the particle positioning within a PS-*b*-P2VP template as a function of Σ. Figure 3 shows the histograms of the particle position of (a) the PS-Au 2.38, (b) PS-Au 1.46, (c) PS-Au 1.06, and (d) PS-Au 0.92 within PS-*b*-P2VP diblock copolymer domains. All histograms were obtained from TEM micrographs of samples containing low ϕ_P (< 0.10) of Au nanoparticles to prevent the disruption of the neat PS-*b*-P2VP lamellar mesophase, thus providing accurate statistics concerning the particle distribution. The histogram in Figure 3a clearly shows that PS-Au 2.38 particles are dispersed within a PS domain of PS-*b*-P2VP block copolymer. As Σ decreases to 1.46 chains/nm^2, the height of the peak near the PS domain center decreases, and a peak appears at the interface between the PS and P2VP domains as shown in Figure 3b. The number of particles at the interface continues to increase further at $\Sigma = 1.06$ chains/nm^2 relative to those in the center of the PS domain, as shown in Figure 3c. We believe that the intermediate behavior of PS-Au 1.46 and PS-Au 1.06, which show particles both at the PS/P2VP interface and the PS domain center, is mainly due to the fact that the mean number $\langle n \rangle$ of

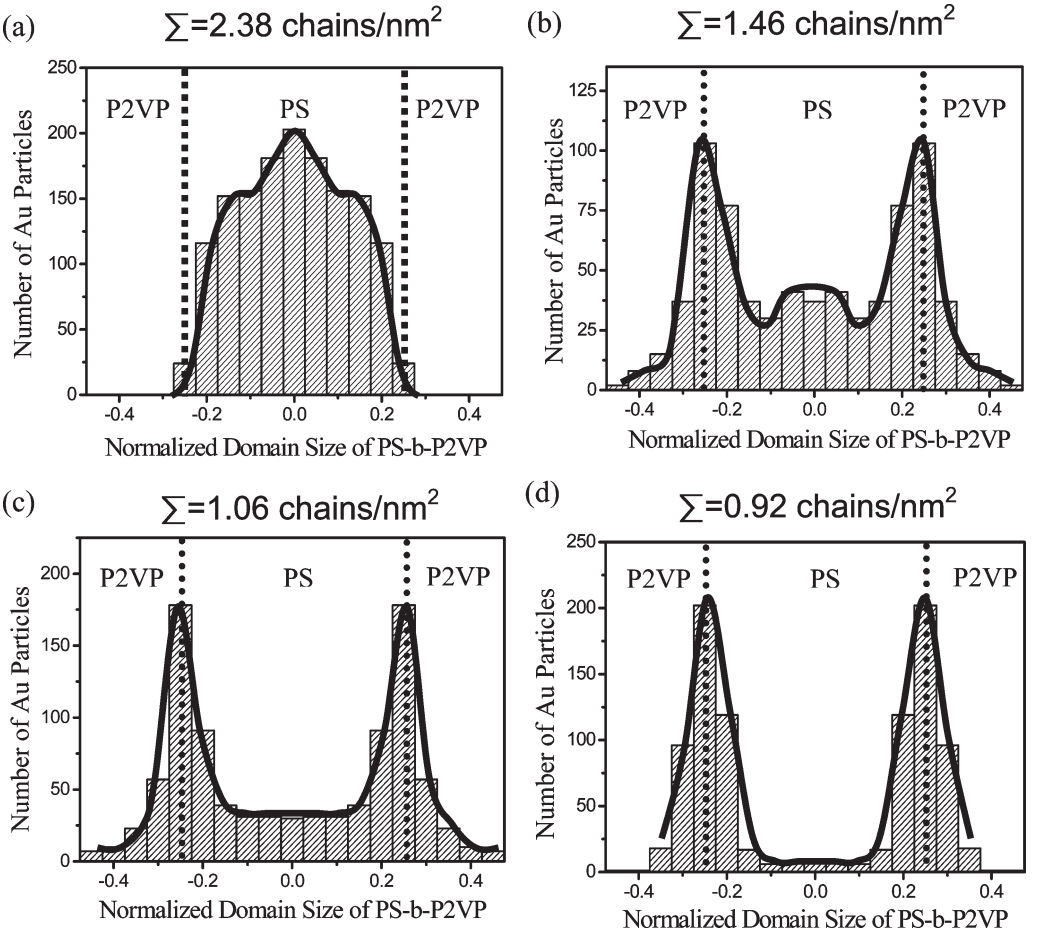

Figure 3. Histograms of the nanoparticle positions of (a) the PS-Au 2.38, (b) PS-Au 1.46, (c) PS-Au 1.06, and (d) PS-Au 0.92 nanoparticles within the lamellar PS-*b*-P2VP block copolymer. Since the PS domain of PS-*b*-P2VP is normalized to 0.5, the center of PS domain is at 0 and the interfaces of the PS domain are at -0.25 and $+0.25$.

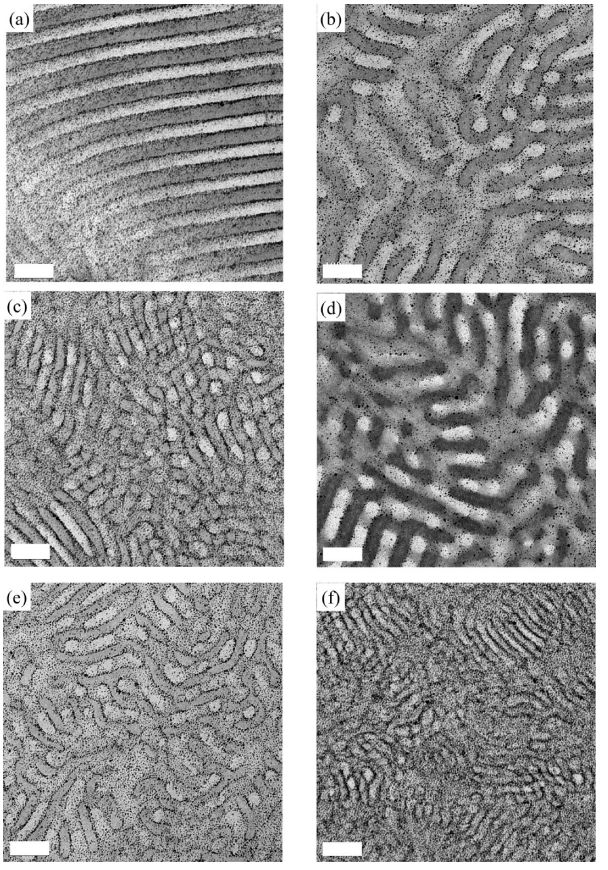

Figure 4. Cross-sectional TEM images of PS-*b*-P2VP block copolymer (M_n = 196 kg/mol) containing PS-Au 0.73 nanoparticles at different ϕ_P = (a) 0.043, (b) 0.048, (c) 0.067, (d) 0.087, (e) 0.095, and (f) 0.192. Scale bar is 100 nm.

PS-SH chains bound to these small Au particles is quite small. If a critical local areal chain density on a given particle exists below which segregation to the interface occurs, a Poisson distribution of n from particle to particle accounts quite well for the particle distributions observed in the histograms as described in our previous papers.[29,43] Finally, PS-Au 0.92 particles are nearly completely segregated to the PS/P2VP interface as shown in Figure 3d. To quantify the histograms, a parameter f_i, the fraction of particles bound to the PS/P2VP interface, is introduced. It is found that f_i values for PS-Au 1.46, PS-Au 1.06, PS-Au 0.97, and PS-Au 0.92 particles are 0.63, 0.74, 0.79, and 0.93, respectively. Therefore, as Σ decreases from 2.38 to 1.46 chains/nm^2, at relatively high $\phi_P \sim 0.25$, the macrophase-separated particle-enriched phase is strongly suppressed, since the particle fraction dispersed in PS domains decreases by a factor of 0.37 (= 1−0.63). As f_i increases further to 0.74, at $\phi_P \sim 0.23$, the particle aggregates within the PS block copolymer domains disappear.

Figure 4 shows representative cross-sectional TEM images of the PS-*b*-P2VP block copolymer (M_n = 196 kg/mol) containing PS-Au 0.73 nanoparticles with various ϕ_P = (a) 0.043, (b) 0.048, (c) 0.067, (d) 0.087, (e) 0.095, and (f) 0.192. A well-ordered lamellar microstructure is seen with the gold nanoparticles (dark dots) segregated at the interfaces between the PS and P2VP domains at ϕ_P = 0.043 (Figure 4a). As the volume fraction of PS-Au 0.73 nanoparticles is increased, the microstructure of the PS-*b*-P2VP diblock copolymer changes dramatically. Figures 4c,d show that when 6.7 and 8.7 vol % of the PS-SH-coated nanoparticles are added, the microstructure of the PS and P2VP domains is drastically changed, becoming bicontinuous. The PS-Au 0.73 nanoparticles cause a uniform disruption of the block copolymer lamellar phase without any sign of macrophase separation. It is remarkable that bicontinuous microstructures are found over an extremely wide range of experimental conditions up to $\phi_P \sim 0.5$ without particle aggregation. Representative TEM images of PS-*b*-P2VP domains for ϕ_P = 0.095 and 0.192 are shown in Figures 4e,f and demonstrate further the surprisingly uniform scale of the bicontinuous structure. Note the dramatic decrease in domain spacing between parts a and f of Figure 4. The normalized domain spacing (h/h_0) of PS-*b*-P2VP diblock copolymers (h_0 is the domain spacing of the pure diblock) is decreased to 0.5, as ϕ_P is increased up to 0.192 in Figure 4f. A decrease in domain size of the block copolymer with ϕ_P reflects a decrease in interfacial tension upon nanoparticle addition and a concomitant increase in block copolymer interfacial area. At the same time, this decrease in domain size indicates that nanoparticles bound to the PS/P2VP interface behave as surfactants at the block copolymer interface. This decrease in domain spacing and thus increase in interfacial area cannot be due to nanoparticle "jamming" since even if one assumes that all nanoparticles are localized at the interface, the nanoparticle area fraction (a_f) is never above 0.5 before the transition to the bicontinuous morphology occurs, and large increases in interfacial area and decreases in lamellar thickness are observed at a_f as low as 0.2. Therefore, the mechanism of bicontinuous phase formation in our system (diblock copolymer/nanoparticles) is believed to be different from that hypothesized for the blending of two homopolymers and particles.[17,19] We will discuss the mechanism based on a recent strong segregation theory.[48]

To investigate further the effect of PS-Au having various Σ values on block copolymer morphology and to further investigate their role as nanoparticle surfactants, PS-coated gold particles with various Σ values were added to the PS-*b*-P2VP block copolymer template. Figure 5 shows cross-sectional TEM images of the PS-*b*-P2VP block copolymer containing PS-Au 0.97 nanoparticles at various ϕ_P = (a) 0.053, (b) 0.103, (c) 0.125, and (d) 0.173. Similar to the TEM images shown in Figure 4, Figure 5 shows that the lamellar microstructure of the PS-*b*-P2VP is disrupted by adding nanoparticles, forming bicontinuous morphologies with uniform spaced domains as ϕ_P increases. The normalized domain spacing (h/h_0) of the PS-*b*-P2VP diblock

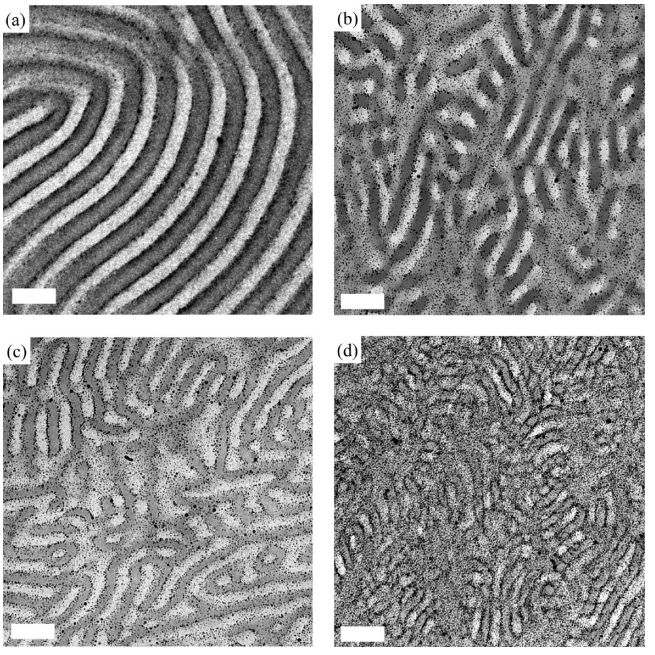

Figure 5. Cross-sectional TEM images of PS-*b*-P2VP block copolymer (M_n = 196 kg/mol) containing PS-Au 0.97 nanoparticles at various ϕ_P values = (a) 0.053, (b) 0.103, (c) 0.125, and (d) 0.173. Scale bar is 100 nm.

copolymer decreases from (a) $h/h_0 = 0.91 \pm 0.05$ at $\phi_P = 0.053$ to (d) $h/h_0 = 0.57 \pm 0.08$ at $\phi_P = 0.173$, which is a trend similar to that observed in Figure 4. Once Σ of PS-SH chains on PS-Au is decreased below a critical value (Σ_C), so that a large fraction of Au particles is strongly bound to the PS/P2VP interface, the transition of morphology from lamellar to bicontinuous is consistently observed as ϕ_P increases. In addition, the threshold particle volume fraction for this transition decreases as Σ of the PS chains on the PS-Au nanoparticles increases.

Discussion

A deeper insight into the morphological transition caused by these nanoparticle surfactants can be gleaned by examination of the normalized domain spacing change (h/h_0) as a function of the particle volume fraction (ϕ_P). Figure 6a represents a two-dimensional morphology diagram, which summarizes the decrease observed in the normalized domain spacing of block copolymer morphology for PS-Au particles with different Σ values as ϕ_P increases. The addition of PS-Au particles having a Σ value larger than 1.46 chains/nm^2 to the PS-*b*-P2VP template leads to macrophase separation of a particle-enriched phase from the lamellar PS-*b*-P2VP phase that contains only a small volume fraction of nanoparticles. In contrast, PS-Au particles having Σ less than 1.06 chains/nm^2 induce a transition of the PS-*b*-P2VP

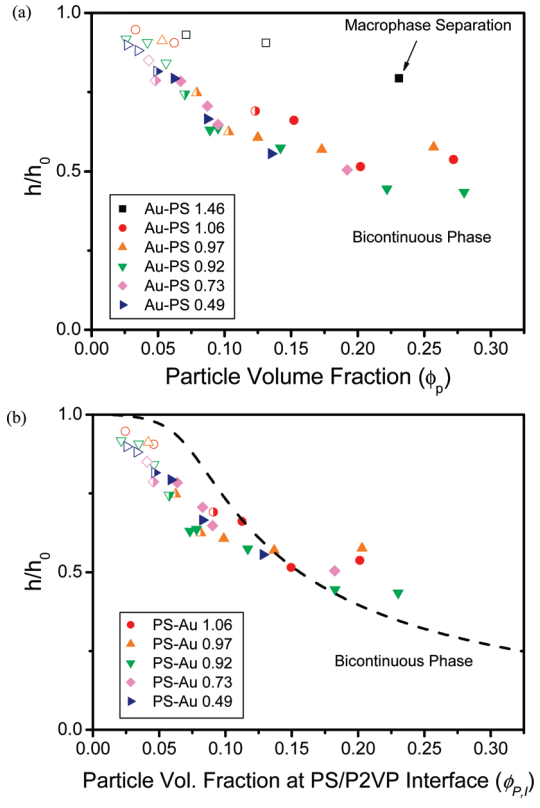

Figure 6. Normalized lamellar domain thickness h/h_0 of the PS-*b*-P2VP diblock copolymer (M_n = 196 kg/mol) versus the total particle volume fraction ϕ_P in (a) and the particle volume fraction localized at the interface $\phi_{P,I}$ in (b). The PS-*b*-P2VP diblock copolymer is mixed with various nanoparticles. (a) PS-Au 1.46 (□), (b) PS-Au 1.06 (○), (c) PS-Au 0.97 (△), (d) PS-Au 0.92 (▽), (e) PS-Au 0.73 (◇), and (f) PS-Au 0.49 (tilted △). While the addition of PS-Au 1.46 nanoparticles eventually results in macrophase-separated structures, the PS-*b*-P2VP morphology with other lower areal chain density particles changes from lamellar (open symbols) to bicontinuous (filled symbols) as ϕ_P increases. The half-filled symbols represent transition morphologies between lamellar and bicontinuous. The dashed line in (b) corresponds to the predictions of a strong segregation theory[48] for 5.7 nm diameter particles segregated to the interface.

lamellar morphology (open symbols) to the bicontinuous structure (filled symbols) as ϕ_P increases. The half-filled symbols represent transition morphologies between lamellar and bicontinuous. The critical particle volume fraction for the transition ($\phi_{P,C}$) decreases as Σ of PS-SH chains on the particles decreases. In addition, the domain spacing of the PS-*b*-P2VP block copolymer decreases dramatically with the addition of the nanoparticle surfactants. Such a decrease in lamellar thickness and increase in interfacial area can be explained qualitatively by a "strong segregation" model[49] of block copolymer morphology. Since the blocks of the block copolymer stretch and lose entropy in order to decrease the interfacial area and thus total energy of the interface between the two blocks, segregation of surfactant nanoparticles to the interface, which leads to a decrease in interfacial tension, allows the stretched blocks to relax and leads to a corresponding decrease in the domain spacing. Interestingly, the recently developed strong segregation theory for surfactant nanoparticles in block copolymers[48] predicts qualitatively many of the features we see in our experiments. This theory by Pyramitsyn and Ganesan[48] considers the free energy of a symmetric diblock copolymer blended with nanoparticles as made up of three terms: the first term represents an entropy loss caused by the block copolymer stretching including the volume excluded by the particles, the second term represents the interfacial cost of blocks and particles, and the third term accounts for the translational entropy of the particles imposed by their density distribution within a block copolymer domain. They predict that the strong contraction in lamellar domain size induces an instability of the lamellar structure beyond $\phi_{P,C}$, leading to a bicontinuous morphology. This theory suggests that the spontaneous bending of the block copolymer brush layer is caused mainly by a near vanishing lamellar bending modulus as ϕ_P approaches $\phi_{P,C}$. Their results bring an interesting comparison to the microemulsion phase of the oil/water/surfactant blends,[50] where the interfacial tension as well as the bending modulus becomes very small. Our morphology is similar to that observed in the system of CPCl/hexanol/brine investigated by Porte et al.[51] However, they report a L_α to L_3 transition of lyotropic surfactants as a result of decrease in the saddle splay modulus.

An analogue of our system (nanoparticle surfactants blends with symmetric diblock copolymers) can be found in the intriguing results of a mixture of two (short and long) lamellar forming diblock copolymers by Hashimoto et al.[52−55] They observed that the interactions between two diblock copolymers, whose covalent linkages share a common interface, can lead to a cosurfactant effect. Such an effect increases interfacial curvature in the case of a blend of two diblock copolymers, which separately would have lamellar morphologies. In such a blend it is possible to form bicontinuous morphologies if the pair is carefully chosen with respect to their molecular weights and block volume fractions.[52,54] In addition to the fact that nanoparticle surfactants share the interface with the junction of block copolymer templates, the nanoparticles may be positioned asymmetrically with respect to the interfacial plane and thus might behave similarly to asymmetric diblock copolymers.[42] In this case the fact that the centers of some particles may be on one side of the interface may strengthen the tendency for formation of a morphology having curved interfaces and a bicontinuous morphology.[56] We believe that such a distortion of the interface would be enhanced due to strong binding of our nanoparticles to the PS/P2VP interface caused by the favorable interaction between the Au bare surface and P2VP block, suppressing the macroscopic separation of a particle-enriched phase.

Since only the fraction f_i of particles bound to the interface (particle surfactants) should be responsible for decreasing the interfacial tension and inducing the morphological transition, the

volume fraction of particles segregated to the interface ($\phi_{P,I} = \phi_P f_i$) should be most relevant for correlating phase behavior. Here f_i can be estimated from the histograms of Figure 3. The normalized domain spacing (h/h_0) for various particles is replotted in terms of $\phi_{P,I}$ in Figure 6b. Plotted as a function of $\phi_{P,I}$ the normalized domain spacing of the diblock copolymer containing various particles with a wide range of Σ values is well described by a single line, indicating that the fraction of particles dispersed in the PS domain, which ranges from 0.05 to 0.27, for Σ values from 0.46 to 1.04 nm^{-2}, does not significantly influence h/h_0. Since small additions of lower molecular weight A homopolymer to A−B diblock copolymers, while increasing the A domain thickness, do not change the overall domain spacing h,[57] the fact that low volume fractions of small nanoparticles in the PS domain do not change h in our system seems reasonable. The predicted h/h_0 of the strong-segregation theory (SST) of Pryamitsyn and Ganesan[48] (the dashed line in Figure 6b) can be compared with the experimental data showing qualitative agreement. There are a number of reasons why we should not expect quantitative agreement, including the fact that the block copolymer/particle system was solvent annealed and thus had ~20 vol % solvent when it vitrified. The SST includes no solvent, and in addition, no account is taken of the PS ligand brush on the nanoparticles.

Figure 7a summarizes the morphology of PS-*b*-P2VP block copolymers containing various PS-Au particles as a function of ϕ_P and Σ, while Figure 7b shows this morphology as a function of $\phi_{P,I}$ and Σ for particles that segregate significantly to the interface. The blend of PS-Au 1.46 nanoparticles and PS-*b*-P2VP changes from lamellar (open symbols) to macrophase-separated PS-Au regions within the block copolymer domains as ϕ_P increases, as shown in Figure 7a. However, the addition of sufficient PS-Au nanoparticles with $\Sigma = 1.06$ chains/nm^2 and less induces a transformation to a bicontinuous morphology of the PS-*b*-P2VP block copolymer indicated by the yellow region in both Figures 7a,b. The critical volume fraction $\phi_{P,I,C}$ for the transition shown in Figure 7b decreases slightly as Σ decreases but not nearly as much as the critical value of the overall volume fraction $\phi_{P,C}$ shown in Figure 7a. As before, it is anticipated that the nanoparticles in the PS domain will have little or no effect on the transition to the bicontinuous morphology. The residual effect of Σ on $\phi_{P,I,C}$ may be caused by the stronger binding of P2VP to the bare Au on nanoparticles with low values of Σ.

We have demonstrated the formation of a bicontinuous morphology of diblock copolymers by addition of various nanoparticle surfactants over an extremely wide range of particle volume fraction. Theoretically, any nanoparticle with an approximately "neutral" surface relative to the A and B polymers will bind to the interface as long as the interfacial tension γ_{AB} of the A/B interface is large enough. For example, a nanoparticle surface covered with chains of random copolymer of A and B will adsorb to such an interface if the composition of A monomers in the copolymers is close to 0.5. However, localization of particles at the interface does not, in itself, guarantee the formation of bicontinuous phase. We believe that the rational design for nanoparticle surfactants having strong binding to the interface is a critical requirement to avoid macroscopic phase separation and obtain a bicontinuous morphology. To prove this concept, we prepared Au nanoparticles coated with a thiol-terminated random copolymer of styrene and 2-vinylpyridine (PS-*r*-P2VP-SH). The PS-*r*-P2VP-SH ligands, which have a M_n of 3.5 kg/mol and a narrow PDI of 1.1, were synthesized by controlled radical polymerization.[36,44] The PS molar fraction of the random copolymer was 0.5 to approximate a neutral coating on the nanoparticle surface, the particle (core + shell) radius was 4 nm, and the areal density was $\Sigma \sim 1.6$ chains/nm^2. The resulting gold nanoparticles were mixed with PS-*b*-P2VP (M_n = 197 kg/mol) at nanoparticle volume fractions (ϕ_P) of 0.1 and 0.3 and then

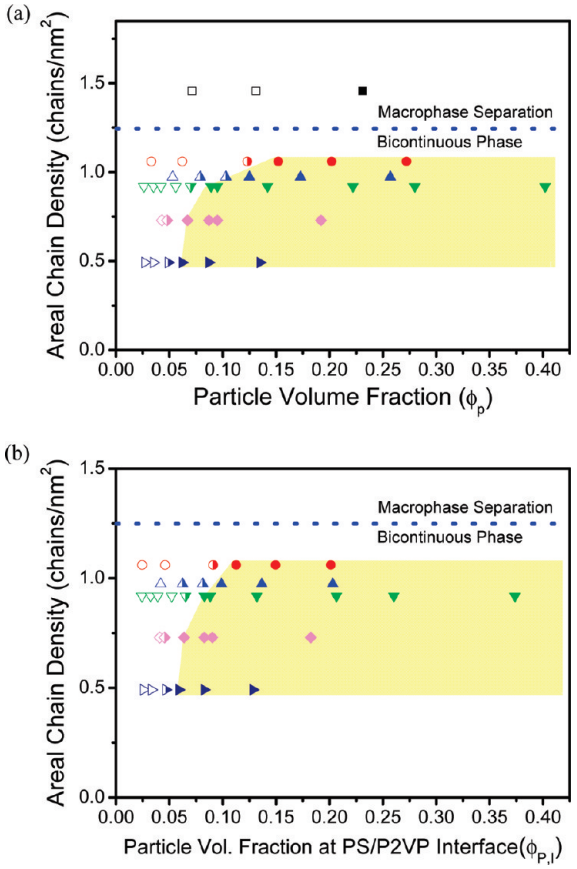

Figure 7. Phase diagram of PS-*b*-P2VP morphologies plotted as a function of Σ of PS-Au particles versus (a) the total volume fraction ϕ_P of gold nanoparticles and (b) the volume fraction $\phi_{P,I}$ of these particles segregated to the interface. The morphology of PS-Au 1.46 nanoparticles/PS-*b*-P2VP changes from lamellar (open symbols) to a macrophase-separated structure consisting of block copolymer domains with some PS-Au 1.46 nanoparticles in the PS domains and the rest in large clusters of PS-Au 1.46 nanoparticles. For nanoparticles with Σ = 1.06 chains/nm^2 or below a transition from a lamellar to a bicontinuous morphology occurs (open symbols: lamellar; half-filled symbols: intermediate; filled symbols: bicontinuous phase).

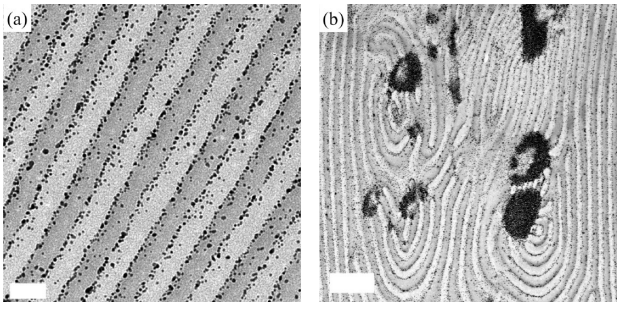

Figure 8. Cross-sectional TEM images of PS-*b*-P2VP block copolymer (M_n = 196 kg/mol) containing PS-*r*-P2VP-coated Au nanoparticles at different ϕ_P: (a) ~0.1 and (b) ~0.3. Scale bars are 50 and 200 nm for (a) and (b), respectively.

solvent annealed as described before. Cross-sectional TEM analysis of the composite at relatively low $\phi_P = 0.1$ in Figure 8a shows ordered lamellar domains with virtually all gold nanoparticles localized at the interfaces. However, the TEM image of PS-*b*-P2VP containing PS-*r*-P2VP-coated particles at $\phi_P \sim 0.3$ (Figure 8b) shows a macroscopically separated particle enriched phase. These results show that the localization of particles to the interface itself is a necessary, but not sufficient, condition to

induce the transition from lamellar to bicontinuous morphology. However, it should be mentioned that TEM analysis reveals a bicontinuous morphology with no macrophase separation when the PS-*r*-P2VP-coated nanoparticles were blended at a composition of $\phi_P \sim 0.15$ with a higher molecular weight block copolymer, symmetric PS-*b*-P2VP (M_n = 380 kg/mol). An increase of the molecular weight of the host matrix reduces the threshold for forming the bicontinuous structure $\phi_{P,C}$ as well as the tendency for macrophase separation as reported in our previous work.[42] The fact that the random copolymer "neutral" surfactant particles are less effective at inducing the bicontinuous morphology than the PS-Au particles with low Σ is probably due to the strong favorable interaction between Au bare surface and P2VP matrix. In addition, since motion of PS chains on the nanoparticle surface is possible by surface diffusion to induce a "Janus" structure, i.e., one with a PS hemispherical surface and a hemispherical surface exposed to P2VP matrix,[36,58,59] stronger adsorption of the PS-Au particles with low Σ to the PS/P2VP interfaces will result. Therefore, the rational design of particles to provide a strong binding to the interface is a critical prerequisite to produce the bicontinuous morphology while suppressing the formation of particle aggregates in the form of a particle-enriched phase.

Conclusions

In summary, the effect of nanoparticle location on the morphology of symmetric diblock copolymers containing polymer-coated nanoparticles was systematically investigated using a model system of PS-*b*-P2VP diblock copolymers and 2.85 nm diameter PS-coated gold nanoparticles. By decreasing the areal density of PS thiol ligands on the nanoparticles the nanoparticles experience an increasingly strong attraction to the interfaces between the two domains of the copolymer. The Σ of PS chains on the nanoparticles is varied from 2.38 to 0.49 chains/nm^2 to produce different fraction of particles localized at the PS/P2VP interface varying from $f_i \sim 0$ to $f_i \sim 0.95$. The addition of a large volume of PS-Au 2.38 particles that are dispersed in the PS domains induced the macroscopic phase separation of a particle-enriched phase from the PS-*b*-P2VP lamellar phase. As f_i is increased by decreasing Σ, macrophase separation is suppressed. When Σ decreases to 1.06 chains/nm^2 and therefore f_i becomes larger than 0.7, a bicontinuous morphology is induced through the incorporation of "nanoparticle surfactants" at the interfaces of the diblock copolymer. The nanoparticle surfactants cause a decrease in both the interfacial tension and the domain spacing and ultimately induce the formation of bicontinuous phase. To demonstrate the importance of the design of the surface coating of the nanoparticles, the morphology of PS-*b*-P2VP copolymers containing "neutral" PS-*r*-P2VP coated particles is compared to that containing PS-coated Au particles with low Σ values. The comparison proves that both particle segregation and strong binding to the interface are important to produce the bicontinuous morphologies.

Acknowledgment. We acknowledge the support of the UCSB Materials Research Laboratory (NSF-DMR-MRSEC Grant DMR05-20415). We thank Prof. Venkat Ganesan for stimulating discussions and providing us a Mathematica file to produce the curve of domain spacing change in block copolymers used in Figure 6b and the skillful help of Dr. Jan P. Löfvander during the TEM experiments.

References and Notes

(1) Klempner, D. *Angew. Chem., Int. Ed. Engl.* **1978**, *17* (2), 97–106.
(2) Hsieh, K. H.; Han, J. L. *J. Polym. Sci., Part B: Polym. Phys.* **1990**, *28* (5), 623–630.
(3) Chen, L.; Phillip, W. A.; Cussler, E. L.; Hillmyer, M. A. *J. Am. Chem. Soc.* **2007**, *129* (45), 13786–13787.
(4) Crossland, E. J. W.; Kamperman, M.; Nedelc, M.; Ducati, C.; Wiesner, U.; Smilgies, D. M.; Toombes, G. E. S.; Hillmyer, M. A.; Ludwigs, S.; Steiner, U.; Snaith, H. A. *Nano Lett.* **2009**, ASAP.
(5) Zhou, N.; Bates, F. S.; Lodge, T. P. *Nano Lett.* **2006**, *6* (10), 2354–2357.
(6) Ma, W. L.; Yang, C. Y.; Gong, X.; Lee, K.; Heeger, A. J. *Adv. Funct. Mater.* **2005**, *15* (10), 1617–1622.
(7) Shaheen, S. E.; Brabec, C. J.; Sariciftci, N. S.; Padinger, F.; Fromherz, T.; Hummelen, J. C. *Appl. Phys. Lett.* **2001**, *78* (6), 841–843.
(8) Yu, G.; Gao, J.; Hummelen, J. C.; Wudl, F.; Heeger, A. J. *Science* **1995**, *270* (5243), 1789–1791.
(9) Bates, F. S.; Maurer, W. W.; Lipic, P. M.; Hillmyer, M. A.; Almdal, K.; Mortensen, K.; Fredrickson, G. H.; Lodge, T. P. *Phys. Rev. Lett.* **1997**, *79* (5), 849–852.
(10) Chan, V. Z. H.; Hoffman, J.; Lee, V. Y.; Iatrou, H.; Avgeropoulos, A.; Hadjichristidis, N.; Miller, R. D.; Thomas, E. L. *Science* **1999**, *286* (5445), 1716–1719.
(11) Hashimoto, T.; Tsutsumi, K.; Funaki, Y. *Langmuir* **1997**, *13* (26), 6869–6872.
(12) Hillmyer, M. A.; Maurer, W. W.; Lodge, T. P.; Bates, F. S.; Almdal, K. *J. Phys. Chem. B* **1999**, *103* (23), 4814–4824.
(13) Pernot, H.; Baumert, M.; Court, F.; Leibler, L. *Nat. Mater.* **2002**, *1* (1), 54–58.
(14) Binks, B. P. *Curr. Opin. Colloid Interface Sci.* **2002**, *7* (1−2), 21–41.
(15) Horozov, T. S.; Binks, B. P. *Angew. Chem., Int. Ed.* **2006**, *45* (5), 773–776.
(16) Borrell, M.; Leal, L. G. *Langmuir* **2007**, *23* (25), 12497–12502.
(17) Stratford, K.; Adhikari, R.; Pagonabarraga, I.; Desplat, J. C.; Cates, M. E. *Science* **2005**, *309* (5744), 2198–2201.
(18) Kim, E.; Stratford, K.; Adhikari, R.; Cates, A. E. *Langmuir* **2008**, *24* (13), 6549–6556.
(19) Chung, H.; Ohno, K.; Fukuda, T.; Composto, R. J. *Nano Lett.* **2005**, *5* (10), 1878–1882.
(20) Cates, M. E.; Clegg, P. S. *Soft Matter* **2008**, *4* (11), 2132–2138.
(21) Herzig, E. M.; White, K. A.; Schofield, A. B.; Poon, W. C. K.; Clegg, P. S. *Nat. Mater.* **2007**, *6* (12), 966–971.
(22) White, K. A.; Schofield, A. B.; Binks, B. P.; Clegg, P. S. *J. Phys.: Condens. Matter* **2008**, *20* (49), 494223.
(23) Bockstaller, M. R.; Lapetnikov, Y.; Margel, S.; Thomas, E. L. *J. Am. Chem. Soc.* **2003**, *125* (18), 5276–5277.
(24) Huang, C. M.; Wei, K. H. *Macromolecules* **2008**, *41* (19), 6876–6879.
(25) Kang, H.; Detcheverry, F. A.; Mangham, A. N.; Stoykovich, M. P.; Daoulas, K. C.; Hamers, R. J.; Muller, M.; de Pablo, J. J.; Nealey, P. F. *Phys. Rev. Lett.* **2008**, *100* (14), 148303.
(26) Maria, S.; Susha, A. S.; Sommer, M.; Talapin, D. V.; Rogach, A. L.; Thelakkat, M. *Macromolecules* **2008**, *41* (16), 6081–6088.
(27) Li, Q. F.; He, J. B.; Glogowski, E.; Li, X. F.; Wang, J.; Emrick, T.; Russell, T. P. *Adv. Mater.* **2008**, *20* (8), 1462–1466.
(28) Lin, Y.; Boker, A.; He, J. B.; Sill, K.; Xiang, H. Q.; Abetz, C.; Li, X. F.; Wang, J.; Emrick, T.; Long, S.; Wang, Q.; Balazs, A.; Russell, T. P. *Nature* (*London*) **2005**, *434* (7029), 55–59.
(29) Kim, B. J.; Bang, J.; Hawker, C. J.; Kramer, E. J. *Macromolecules* **2006**, *39* (12), 4108–4114.
(30) Kim, B. J.; Chiu, J. J.; Yi, G. R.; Pine, D. J.; Kramer, E. J. *Adv. Mater.* **2005**, *17* (21), 2618–2622.
(31) Listak, J.; Bockstaller, M. R. *Macromolecules* **2006**, *39* (17), 5820–5825.
(32) Spontak, R. J.; Shankar, R.; Bowman, M. K.; Krishnan, A. S.; Hamersky, M. W.; Samseth, J.; Bockstaller, M. R.; Rasmussen, K. O. *Nano Lett.* **2006**, *6* (9), 2115–2120.
(33) Lan, Q.; Francis, L. F.; Bates, F. S. *J. Polym. Sci., Part B: Polym. Phys.* **2007**, *45* (16), 2284–2299.
(34) Xu, C.; Ohno, K.; Ladmiral, V.; Composto, R. J. *Polymer* **2008**, *49* (16), 3568–3577.
(35) Chiu, J. J.; Kim, B. J.; Kramer, E. J.; Pine, D. J. *J. Am. Chem. Soc.* **2005**, *127* (14), 5036–5037.
(36) Kim, B. J.; Bang, J.; Hawker, C. J.; Chiu, J. J.; Pine, D. J.; Jang, S. G.; Yang, S. M.; Kramer, E. J. *Langmuir* **2007**, *23* (25), 12693–12703.
(37) Tsutsumi, K.; Funaki, Y.; Hirokawa, Y.; Hashimoto, T. *Langmuir* **1999**, *15* (16), 5200–5203.
(38) Walther, A.; Matussek, K.; Muller, A. H. E. *ACS Nano* **2008**, *2* (6), 1167–1178.
(39) Pieranski, P. *Phys. Rev. Lett.* **1980**, *45* (7), 569–572.
(40) Kim, J. U.; Matsen, M. W. *Phys. Rev. Lett.* **2009**, *102* (7), 078303.

(41) Matsen, M. W.; Thompson, R. B. *Macromolecules* **2008**, *41* (5), 1853–1860.
(42) Kim, B. J.; Fredrickson, G. H.; Hawker, C. J.; Kramer, E. J. *Langmuir* **2007**, *23* (14), 7804–7809.
(43) Kim, B. J.; Fredrickson, G. H.; Kramer, E. J. *Macromolecules* **2008**, *41* (2), 436–447.
(44) Drockenmuller, E.; Li, L. Y. T.; Ryu, D. Y.; Harth, E.; Russell, T. P.; Kim, H. C.; Hawker, C. J. *J. Polym. Sci., Part A: Polym. Chem.* **2005**, *43* (5), 1028–1037.
(45) Brust, M.; Walker, M.; Bethell, D.; Schiffrin, D. J.; Whyman, R. *J. Chem. Soc., Chem. Commun.* **1994**, *7*, 801–802.
(46) Yee, C. K.; Jordan, R.; Ulman, A.; White, H.; King, A.; Rafailovich, M.; Sokolov, J. *Langmuir* **1999**, *15* (10), 3486–3491.
(47) Thompson, R. B.; Ginzburg, V. V.; Matsen, M. W.; Balazs, A. C. *Science* **2001**, *292* (5526), 2469–2472.
(48) Pryamitsyn, V.; Ganesan, V. *Macromolecules* **2006**, *39* (24), 8499–8510.
(49) Semenov, A. N. *Zh. Eksp. Teor. Fiz.* **1985**, *88* (4), 1242–1256.
(50) Degennes, P. G.; Taupin, C. *J. Phys. Chem.* **1982**, *86* (13), 2294–2304.
(51) Porte, G.; Appell, J.; Bassereau, P.; Marignan, J. *J. Phys.* (*Paris*) **1989**, *50* (11), 1335–1347.
(52) Hasegawa, H.; Hashimoto, T.; Hyde, S. T. *Polymer* **1996**, *37* (17), 3825–3833.
(53) Hashimoto, T.; Yamaguchi, D.; Court, F. *Macromol. Symp.* **2003**, *195*, 191–200.
(54) Hashimoto, T.; Yamasaki, K.; Koizumi, S.; Hasegawa, H. *Macromolecules* **1993**, *26* (11), 2895–2904.
(55) Yamaguchi, D.; Hashimoto, T. *Macromolecules* **2001**, *34* (18), 6495–6505.
(56) Court, F.; Yamaguchi, D.; Hashimoto, T. *Macromolecules* **2006**, *39* (7), 2596–2605.
(57) Winey, K. I.; Thomas, E. L.; Fetters, L. J. *Macromolecules* **1991**, *24* (23), 6182–6188.
(58) Shan, J.; Nuopponen, M.; Jiang, H.; Viitala, T.; Kauppinen, E.; Kontturi, K.; Tenhu, H. *Macromolecules* **2005**, *38* (7), 2918–2926.
(59) Shan, J.; Tenhu, H. *Chem. Commun.* **2007**, *44*, 4580–4598.